Supporting Information

Twisted diphenoquinones fused with thiophene rings: Thiophene analogs of bianthrone

Yohei Adachi,[1]* Yuto Hattori,[1] Tsubasa Mikie,[2] Itaru Osaka[2] and Joji Ohshita[1,3]*

[1] *Smart Innovation Program, Graduate School of Advanced Science and Engineering, Hiroshima University, Higashi-Hiroshima 739-8527, Japan. E-mail: yadachi@hiroshima-u.ac.jp, jo@hiroshima-u.ac.jp*

[2] *Applied Chemistry Program, Graduate School of Advanced Science and Engineering, Hiroshima University, Higashi-Hiroshima 739-8527, Japan.*

[3] *Division of Materials Model-Based Research, Digital Monozukuri (Manufacturing) Education and Research Center, Hiroshima University, Higashi-Hiroshima, Hiroshima 739-0046, Japan.*

Experimental

Materials

All reactions were carried out under dry argon. For the reaction solvents, diethyl ether, THF, and toluene were purchased from Kanto Chemical Co., Ltd., distilled from calcium hydride, and stored over activated molecular sieves under argon until use. All other chemicals were purchased from FUJIFILM Wako Pure Chemical Corporation or TCI Co., Ltd. Starting materials bis(3-thienyl)methane (compound **1**)[S1] and bis(2-bromo-3-thienyl)methane (compound **3**)[S2] were prepared according to the literature procedure. NMR spectra were recorded on Varian System 500 and 400MR spectrometers. Abbreviations Th and Bz used for the following NMR assignments stand for thiophene and benzene ring, respectively. High-resolution APCI and GC-EI mass spectra were obtained on a Thermo Fisher Scientific LTQ Orbitrap XL spectrometer and a JEOL JMS-T2000GC, respectively, at N-BARD, Hiroshima University. ESR spectra of **dDTCO-Bu** dissolved in benzene (1 mM) were recorded using a Bruker E500 (X-band) spectrometer in the temperature range from 120 K to 240 K, and at 77 K and room temperature. The measurements were performed under the spectrometer settings with a modulation amplitude of 5.0 G at 100 kHz, a conversion time of 60 ms, a total number of data points of 4096, a microwave power of 4 mW, and a magnetic field with of 4000 G at the central field 2500 G. DSC analysis was carried out under gentle nitrogen flow at a heating rate of 10 ºC/min using the SII DSC6200 analyzer.

Photophysical measurements

UV–vis absorption spectra were measured with a HITACHI U-2910 spectrophotometer. The concentration of the samples was 10 μmol/L. A quartz cuvette with an optical path length of 1.0 cm was used for the measurements, and the background was corrected using the double-beam method. The molar absorption coefficient was calculated from the Lambert-Beer law ($A = \varepsilon cl$, A: absorbance, ε: molar absorption coefficient, l: optical path length, c: concentration).

Electrochemical measurements

Cyclic voltammetry measurements were performed with an AMETEK VersaSTAT 4 potentiostat/galvanostat

in a 1.0 mM solution in dichloromethane containing 0.1 M [nBu$_4$N][PF$_6$] at a 100 mV s^{-1} scan rate using a three-electrode system which was composed of a Pt plate as the counter electrode, a Pt wire as the working electrode, and an Ag wire as the pseudo-reference electrode. The potentials were corrected using ferrocene as the internal standard.

DFT calculations

All geometrical optimizations and TD-DFT calculations were performed on a Gaussian 16 program at the B3LYP-D3(BJ)/6-31G(d) level of theory. No imaginary frequencies were found for all the ground state optimized structures, whereas only one imaginary frequency was observed for the TS geometry. The optimization of the twisted conformer of **dDTCO** was also performed for the open-shell singlet state, but it converged to the same structure as the closed-shell singlet state. The intrinsic reaction coordinate (IRC) calculation was performed on the TS structure at the same level to confirm that the transition state connects the twisted and folded conformers. TD-DFT calculations were performed for the 20 lowest singlet and triplet states on the S_0 geometries.

XRD measurements

Single crystal X-ray diffraction data of **dDTCO**/**dDTCO-Me** and **dDTCO-Bu** were collected at 100 K on a Bruker AXS SMART APEX II ULTRA diffractometer and on a Rigaku XtaLAB Synergy-R/DW, respectively, at Natural Science Center for Basic Research and Development (N-BARD), Hiroshima University, using MoKα radiation monochromated with a multilayered confocal mirror. The structure was solved by Intrinsic Phasing on the SHELXT-2014/5 or SHELXT-2018/2 program and expanded using Fourier techniques. Non-hydrogen atoms were refined anisotropically, whereas hydrogen atoms were included but not refined (SHELXL-2018/3). All other calculations were performed using the APEXII crystallographic software package of Bruker AXS or the Olex2 1.3-ac4 software. Graphical crystal structures were generated using Mercury 4.3.1 (Cambridge Crystallographic Data Centre).

OFET fabrication and measurements

Top-gate-bottom-contact (TGBC) devices were fabricated on an alkaline-free glass substrate, where Cr/Au source and drain electrode were patterned via photolithography. The glass substrates were ultrasonicated with isopropanol for 10 min, and rinsed in boiled isopropanol for 10 min, and then were subjected to UV-ozone treatment for 30 min. The cleaned substrates were treated by 1-octanethiol (OT) to modify the Au source and drain electrodes. Thin films of **dDTCO-Bu** and **dDTCB** were spin-coated from 5 mg mL^{-1} chloroform solutions. Since the high-temperature annealing caused the thin film of **dDTCO-Bu** to discolor, suggesting the degradation, annealing was conducted at a relatively low temperature of 100 °C for 10 min. The CYTOP dielectric layer (C_i = 4.13 nF cm^{-2}) with ca. 450 nm thickness was spin-coated on top of the active layer and then was dried at r.t for 12 h. Finally, the Ag layer (100 nm) was evaporated on top as the gate electrode through a shadow mask. Current-voltage characteristics were measured at room temperature under vacuum conditions with a KEYSIGHT B2902A and a semiconductor parameter analysis software (SYSTEMHOUSE SUNRISE). Threshold voltages were estimated from the transfer plots by extrapolating the square root of the drain current to the horizontal axis. Electron field-effect mobilities were extracted from the square root of the drain current in the saturation regime by using the following equation,

$$\mu = \frac{2L}{WC_i}\left(\frac{d\sqrt{|I_d|}}{dV_g}\right)^2$$

where, L (25 μm) and W (10000 μm) are channel length and width, respectively, and C_i is capacitance of the gate insulator. The average hole and electron mobilities and threshold voltages were obtained over more than eight devices.

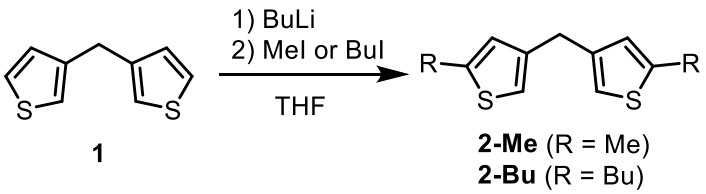

1

2-Me (R = Me)
2-Bu (R = Bu)

*Synthesis of **2-Me***

To a solution of 3.78 g (21.0 mmol) of **1** in 150 mL of THF was added 15.8 mL (42.0 mmol) of 2.66 mol/L BuLi in hexane at 0 °C over a period of 10 min and the mixture was stirred at this temperature for 1 h. To this was added 3.71 mL (59.6 mmol) of iodomethane at –78 °C and the mixture was stirred at room temperature overnight. The resulting mixture was hydrolyzed with water, and 200 mL of hexane was added. The organic

layer was separated, and the aqueous layer was extracted with 100 mL of hexane. The combined organic layers were washed with water and then with brine. After drying over anhydrous magnesium sulfate, the solvent was evaporated. The crude product was purified by silica gel chromatography using *n*-hexane as the eluent to give 2.97 g (14.3 mmol, 68% yield) of **2-Me** as a colorless oil. The obtained product contained a small amount of impurities that could not be separated, but was used as is in the next step. The ^{1}H NMR data of the major peaks matched the literature values.[S3]

*Synthesis of **2-Bu***

Compound **2-Bu** was prepared from 3.81 g (21.1 mmol) of **1**, 16.0 mL (42.2 mmol) of 2.64 mol/L BuLi in hexane, 6.84 mL (60.2 mmol) of 1-iodobutane, 120 mL of THF as a colorless oil (4.27 g, 14.6 mmol, 69% yield) in a manner similar to that above. The obtained product contained a small amount of impurities that could not be separated, but was used as is in the next step. ^{1}H NMR (500 MHz, $CDCl_3$) δ 6.73 (s, 2H, Th), 6.65 (s, 2H, Th), 3.85 (s, 2H, methylene), 2.84–2.75 (m, 4H, *n*Bu), 1.71–1.63 (m, 4H, *n*Bu), 1.47–1.38 (m, 4H, *n*Bu), 1.00–0.92 (m, 6H, *n*Bu). ^{13}C{^{1}H} NMR (126 MHz, $CDCl_3$) δ 145.9, 140.6, 125.5, 118.4, 33.8, 31.7, 29.8, 22.2, 13.8. HRMS (GC-EI) Calcd. for $C_{17}H_{24}S_2$: M^+: 292.13139, Found: 292.13079.

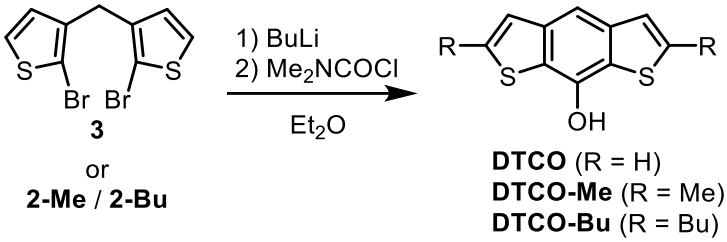

*Synthesis of **DTCO***

To a solution of 6.31 g (18.7 mmol) of **3** in 60 mL of Et_2O was added 16.5 mL (43.9 mmol) of 2.66 mol/L BuLi in hexane at –78 °C over a period of 20 min and the mixture was stirred at this temperature for 1 h. To this was added 1.73 mL (18.8 mmol) of dimethylcarbamoyl chloride in 30 mL of Et_2O at this temperature and the mixture was stirred at room temperature overnight. The resulting mixture was hydrolyzed with saturated NH_4Cl aqueous solution, and 100 mL of ethyl acetate was added. The organic layer was separated, and the aqueous layer was extracted with 50 mL of ethyl acetate. The combined organic layers were washed with

water and then with brine. After drying over anhydrous magnesium sulfate, the solvent was evaporated. The crude product was purified by silica gel chromatography using dichloromethane as the eluent to give 1.53 g (7.42 mmol, 40% yield) of **DTCO** as a white solid. The obtained product was used immediately for the next reaction as it was gradually oxidized in air. ^{1}H NMR (400 MHz, DMSO-d_6) δ 10.60 (s, 1H, OH), 7.92 (s, 1H, Bz), 7.68 (d, J = 5.4 Hz, 2H, Th), 7.46 (d, J = 5.4 Hz, 2H, Th). ^{13}C{^{1}H} NMR (101 MHz, DMSO-d_6) δ 145.6, 139.9, 127.0, 124.3, 123.2, 109.8. HRMS (APCI, positive) Calcd. for $C_{10}H_7OS_2$: $[M+H]^+$: 206.99328, Found: 206.99303. m.p. 122 ℃ (DSC).

*Synthesis of **DTCO-Me***

To a solution of 2.97 g (14.3 mmol) of **2-Me** in 20 mL of THF was added 10.5 mL (27.9 mmol) of 2.66 mol/L BuLi in hexane at –78 ℃ over a period of 15 min and the mixture was stirred at 0 ℃ for 1 h. To this was added 1.32 mL (14.4 mmol) of dimethylcarbamoyl chloride in 10 mL of THF at –78 ℃ and the mixture was stirred at room temperature overnight. After workup and purification in a manner similar to that above, **DTCO-Me** was obtained as a white solid (0.657 g, 2.80 mmol, 20% yield). The obtained product was used immediately for the next reaction as it was gradually oxidized in air. ^{1}H NMR (400 MHz, DMSO-d_6) δ 10.32 (s, 1H, OH), 7.57 (s, 1H, Bz), 7.10–7.06 (m, 2H, Th), 2.54 (d, J = 1.1 Hz, 6H, CH_3). ^{13}C{^{1}H} NMR (101 MHz, DMSO-d_6) δ 145.0, 140.7, 140.2, 122.7, 122.6, 108.5, 16.5. HRMS (APCI, positive) Calcd. for $C_{12}H_{11}OS_2$: $[M+H]^+$: 235.02458, Found: 235.02477. m.p. 153 ℃ (DSC).

*Synthesis of **DTCO-Bu***

Compound **DTCO-Bu** was prepared from 1.07 g (3.66 mmol) of **2-Bu**, 2.77 mL (7.31 mmol) of 2.64 mol/L BuLi in hexane, 0.314 mL (3.42 mmol) of dimethylcarbamoyl chloride, 10 mL of THF as a white solid (0.331 g, 1.04 mmol, 28% yield) in a manner similar to that above. The obtained product was used immediately for the next reaction as it was gradually oxidized in air. ^{1}H NMR (500 MHz, $CDCl_3$) δ 7.61 (s, 1H, Bz), 7.01 (s, 2H, Th), 5.04 (br s, 1H, OH), 2.91 (t, J = 7.57 Hz, 4H, *n*Bu), 1.79–1.71 (m, 4H, *n*Bu), 1.48–1.40 (m, 4H, *n*Bu), 0.96 (t, J = 7.4 Hz, 6H, *n*Bu). ^{13}C{^{1}H} NMR (126 MHz, $CDCl_3$) δ: 145.9, 143.4, 140.5, 121.9, 121.0, 109.5, 33.1, 30.7, 22.2, 13.8. HRMS (GC-EI) Calcd. for $C_{18}H_{22}OS_2$: M^+: 318.11066, Found: 318.11155. m.p. 91 ℃

(DSC).

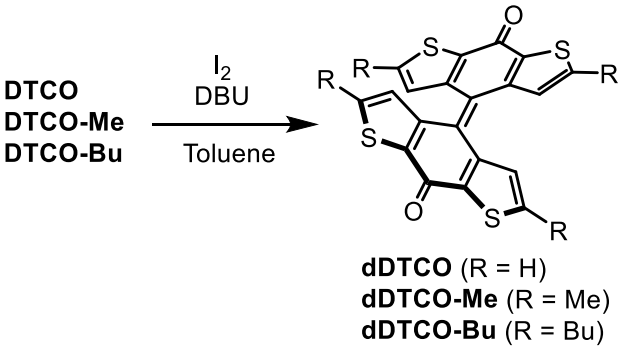

*Synthesis of **dDTCO***

To a solution of **DTCO** (100 mg, 0.485 mmol) and I_2 (123 mg, 0.485 mmol) in 5 mL of toluene was added 145 μL (0.970 mmol) of DBU at room temperature and the mixture was stirred overnight. The resulting mixture was hydrolyzed with sodium thiosulfate aqueous solution and extracted with 100 mL of CH_2Cl_2. The organic layer was washed once with water then with brine. After drying over anhydrous magnesium sulfate, the solvent was evaporated. The crude product was washed with methanol to give 62.2 mg (0.152 mmol, 63 % yield) of **dDTCO** as a dark blueish powder. ^{1}H NMR (500 MHz, CD_2Cl_2) δ 7.56 (d, J = 5.3 Hz, 4H, Th), 7.53 (d, J = 5.3 Hz, 4H, Th). ^{13}C{^{1}H} NMR (126 MHz, CD_2Cl_2) δ 173.0, 143.8, 140.6, 133.4, 131.4, 130.5. HRMS (APCI, positive) Calcd for $C_{20}H_9O_2S_4$: $[M+H]^+$: 408.94799, Found 408.94781. m.p. >300 ℃.

*Synthesis of **dDTCO-Me***

Compound **DTCO-Me** was prepared from 102 mg (0.435 mmol) of **DTCO-Me**, 108 mg (0.426 mmol) of I_2, 128 μL (0.856 mmol) of DBU, 5 mL of toluene as a dark blueish powder (76.5 mg, 0.165 mmol, 76% yield) in a manner similar to that above. ^{1}H NMR (400 MHz, $CDCl_3$) δ: 7.18–7.15 (m, 4H, Th), 2.47 (d, J = 1.0 Hz, 12H, CH_3). ^{13}C{^{1}H} NMR (126 MHz, $CDCl_3$) δ: 172.2, 145.7, 143.4, 138.6, 132.6, 128.0, 16.3. HRMS (APCI, positive) Calcd. for $C_{24}H_{17}O_2S_4$: $[M+H]^+$: 465.01059, Found: 465.01096. m.p. >300 ℃.

*Synthesis of **dDTCO-Bu***

Compound **DTCO-Bu** was prepared from 100 mg (0.314 mmol) of **DTCO-Bu**, 79.8 mg (0.314 mmol) of I_2, 93.8 μL (0.627 mmol) of DBU, 5 mL of toluene as a dark blueish powder (69.4 mg, 0.110 mmol, 70% yield)

in a manner similar to that above. ^{1}H NMR (500 MHz, $CDCl_3$) δ 7.20 (s, 4H, Th), 2.75 (t, J = 7.5 Hz, 8H, *n*Bu), 1.67–1.58 (m, 8H, *n*Bu), 1.40–1.31 (m, 8H, *n*Bu), 0.90 (t, J = 7.4 Hz, 12H, *n*Bu). ^{13}C{^{1}H} NMR (126 MHz, $CDCl_3$) δ 172.2, 151.5, 143.2, 138.3, 132.6, 127.1, 33.2, 30.4, 22.0, 13.7. HRMS (GC-EI) Calcd. for $C_{36}H_{40}O_2S_4$: M^+: 632.19056, Found: 632.19173. m.p. >300 ℃.

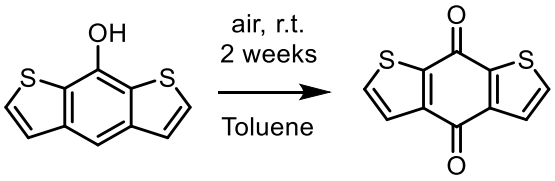

Air oxidation of ***DTCO***

DTCO was dissolved in toluene and stirred in air for two weeks. After removal of the solvent, the quinone was obtained quantitatively. ^{1}H NMR (500 MHz, $CDCl_3$) δ 7.68 (d, J = 5.0 Hz, 2H, Th), 7.63 (d, J = 5.0 Hz, 2H, Th). ^{13}C{^{1}H} NMR (126 MHz, $CDCl_3$) δ 175.8, 173.2, 144.7, 142.7, 133.7, 126.7.

References

[S1] J. C. Bijleveld, M. Shahid, J. Gilot, M. M. Wienk, R. A. J. Janssen, *Adv. Funct. Mater.*, 2009, **19**, 3262.

[S2] Y. Adachi, T. Nomura, S. Tazuhara, H. Naito and J. Ohshita, *Chem. Commun.*, 2021, **57**, 1316.

[S3] I. E. Nifant'ev, A. A. Vinogradov, A. A. Vinogradov, G. I. Sadrtdinova, P. D. Komarov, M. E. Minyaev, S. O. Ilyin, A. V. Kiselev, T. I. Samurganova, P. V. Ivchenko, *Eur. Polym. J.*, 2022, **176**, 111397.

Figures and Tables

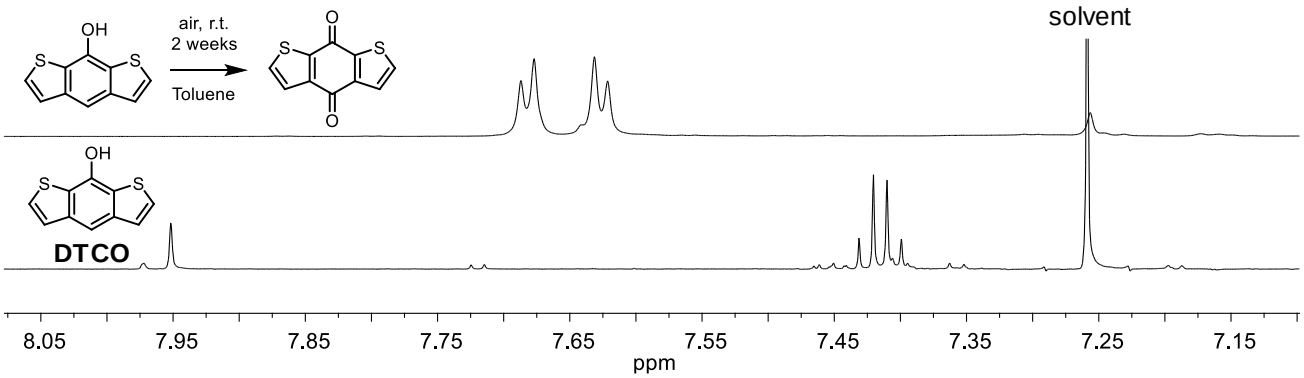

Fig. S1 Partial ^{1}H NMR spectra of **DTCO** and dithienobenzoquinone in $CDCl_3$.

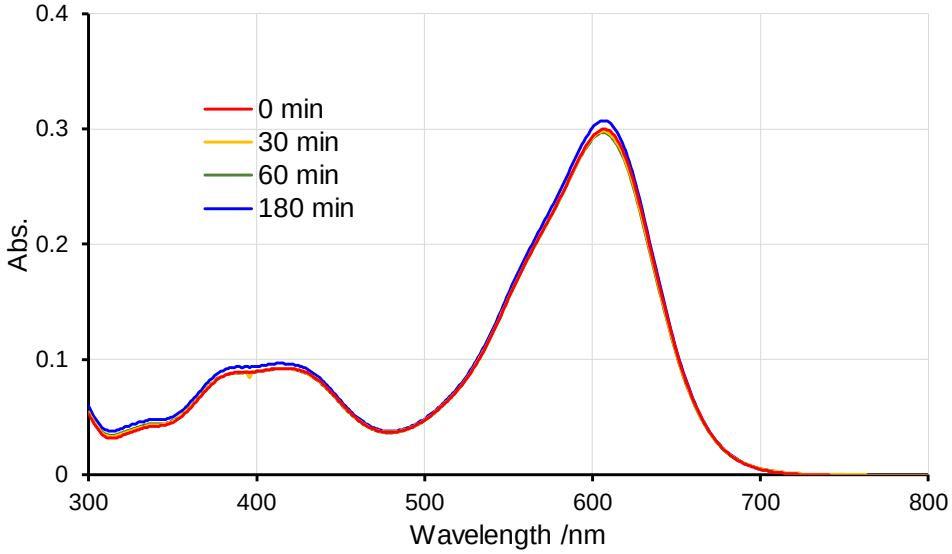

Fig. S2 UV-vis absorption spectral changes of **dDTCO** in CH_2Cl_2 toward the irradiation of UV light (365 nm) using a 4 W, 365 nm hand-held UV lamp.

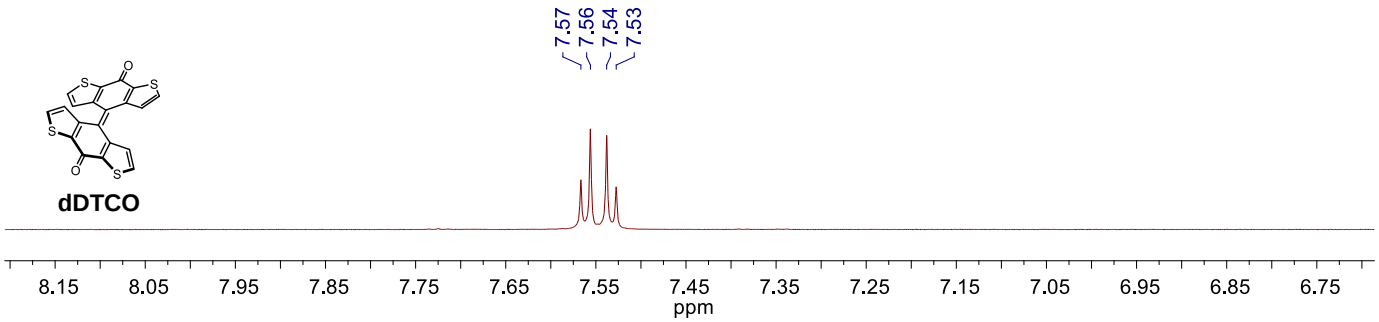

Fig. S3 Partial ^{1}H NMR spectrum of **dDTCO** in the aromatic region in CD_2Cl_2.

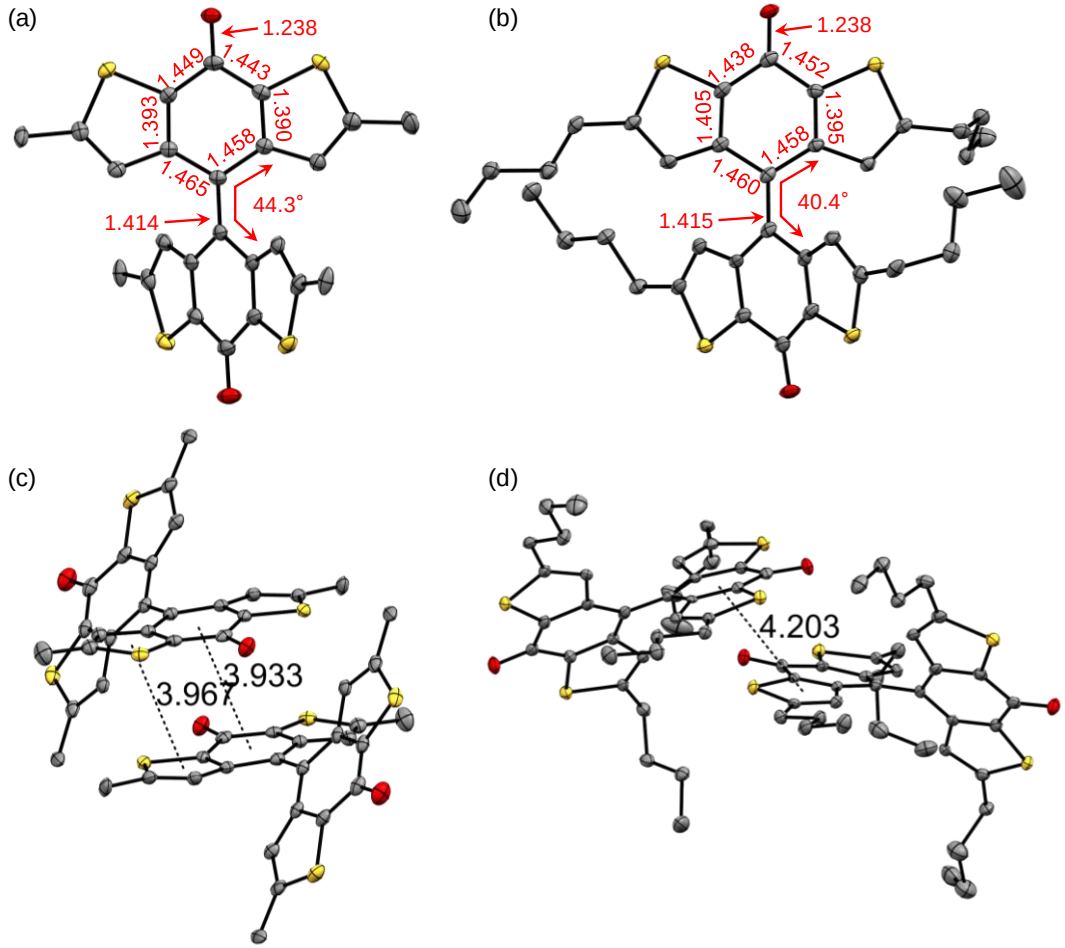

Fig. S4 Single-crystal X-ray structures of the monomers (a) **dDTCO-Me** and (b) **dDTCO-Bu**, and the dimers (c) **dDTCO-Me** and (d) **dDTCO-Bu** obtained at 100 K. Thermal ellipsoids are at the 50% probability level. Hydrogen atoms are omitted for clarity.

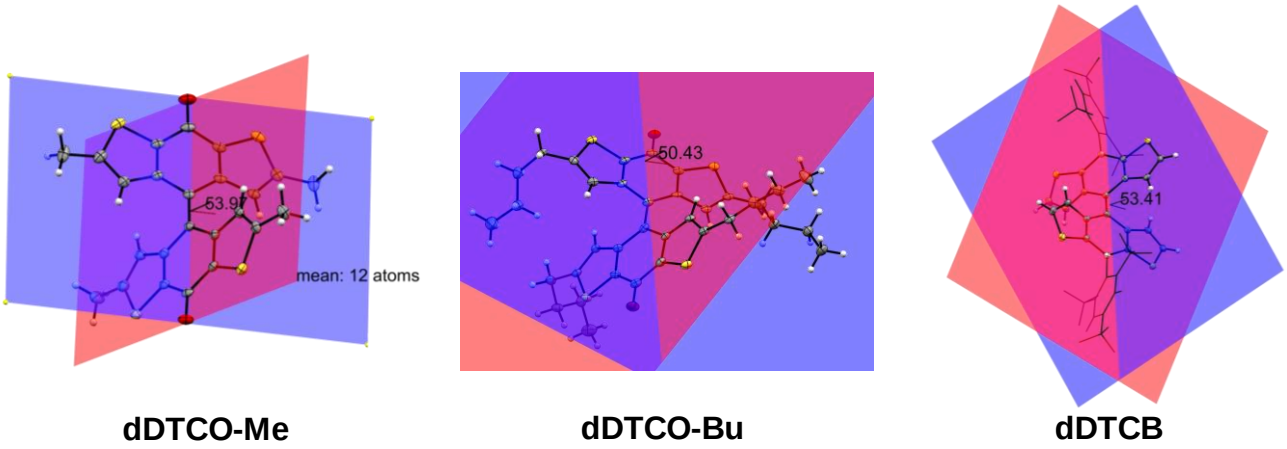

Fig. S5 Dihedral angle between the mean planes of the 12 atoms of the tricyclic structures.

Table S1 Bond lengths in Å and dihedral angle obtained from single-crystal X-ray structures.

Bond	**dDTCO**	**dDTCO-Me**	**dDTCO-Bu**	Bianthrone
C1-O	1.233(3)	1.238(3)	1.238(4)	1.224(1)
C1-C2	1.457(3)	1.443(4)	1.452(4)	1.486(1)
C2-C3	1.396(4)	1.390(4)	1.395(5)	1.411(1)
C3-C4	1.455(5)	1.458(4)	1.458(5)	1.493(2)
C4-C5	1.456(3)	1.465(4)	1.460(4)	1.493(1)
C5-C6	1.392(4)	1.393(4)	1.405(5)	1.407(2)
C6-C1	1.450(5)	1.449(4)	1.438(5)	1.491(2)
C4-C7	1.413(4)	1.414(4)	1.415(5)	1.362(1)
Dihedral (C3-C4=C7-C8)	44.8(4)°	44.3(4)°	40.4(5)°	4.2(2)°

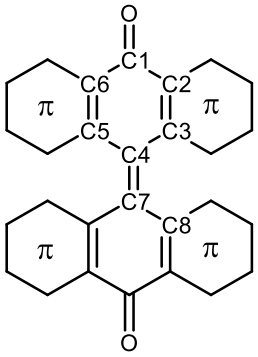

The numbering of the carbon atoms does not follow the IUPAC standard for clarity.

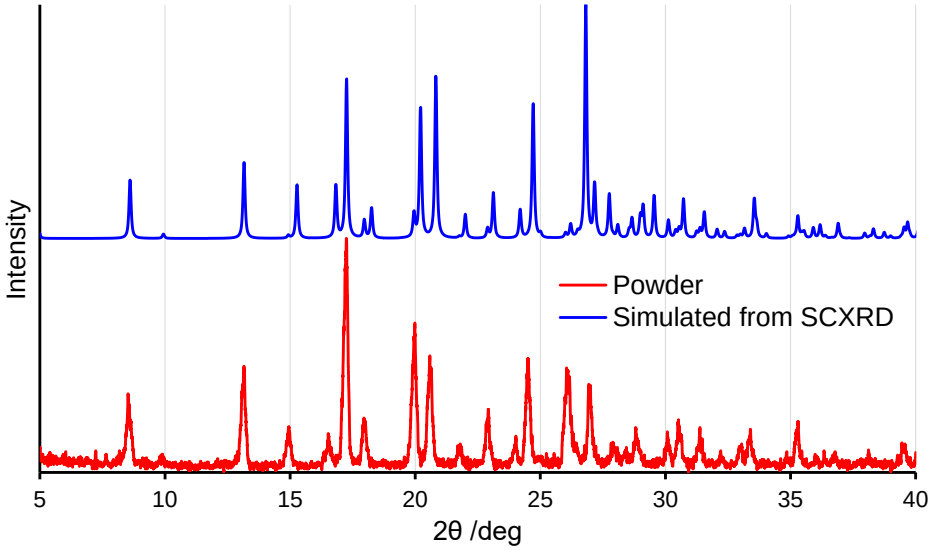

Fig. S6 XRD patterns of a powder of recorded at r.t. and simulated patterns from the single crystal XRD measured at 100 K for **dDTCO**.

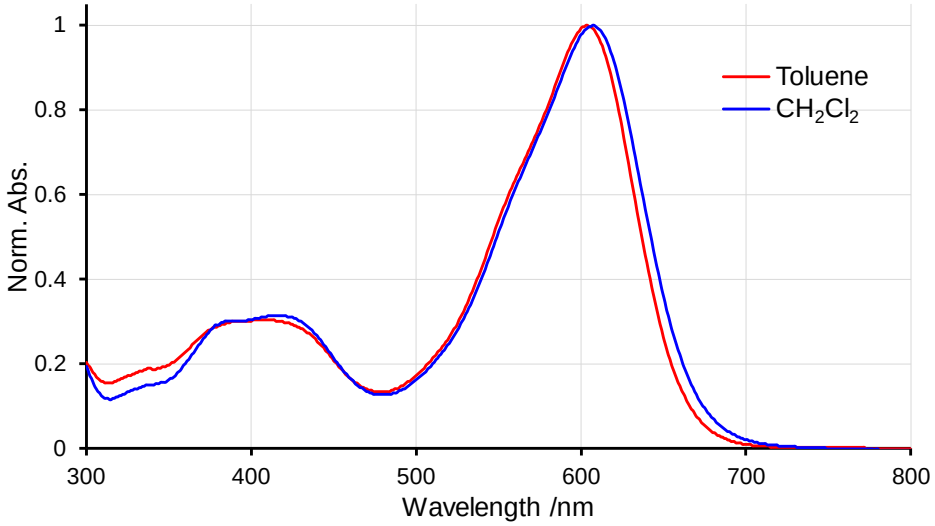

Fig. S7 UV UV-vis absorption spectra of **dDTCO** in toluene and CH_2Cl_2 at the concentration of 0.01 mM.

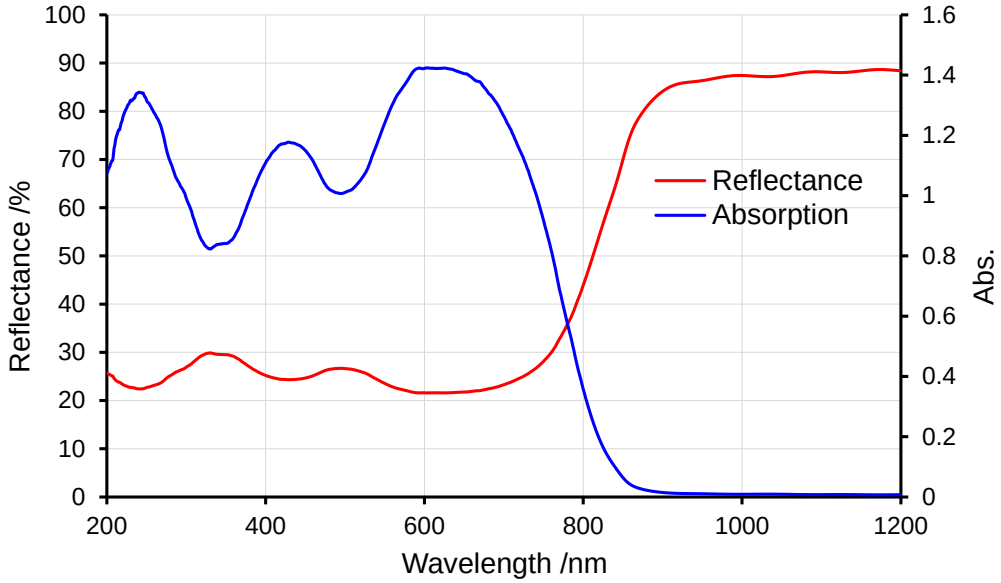

Fig. S8 Diffuse reflectance spectrum of **dDTCO** in the solid state. The diffuse reflection spectrum was converted into absorption by using the Kubelka-Munk equation.

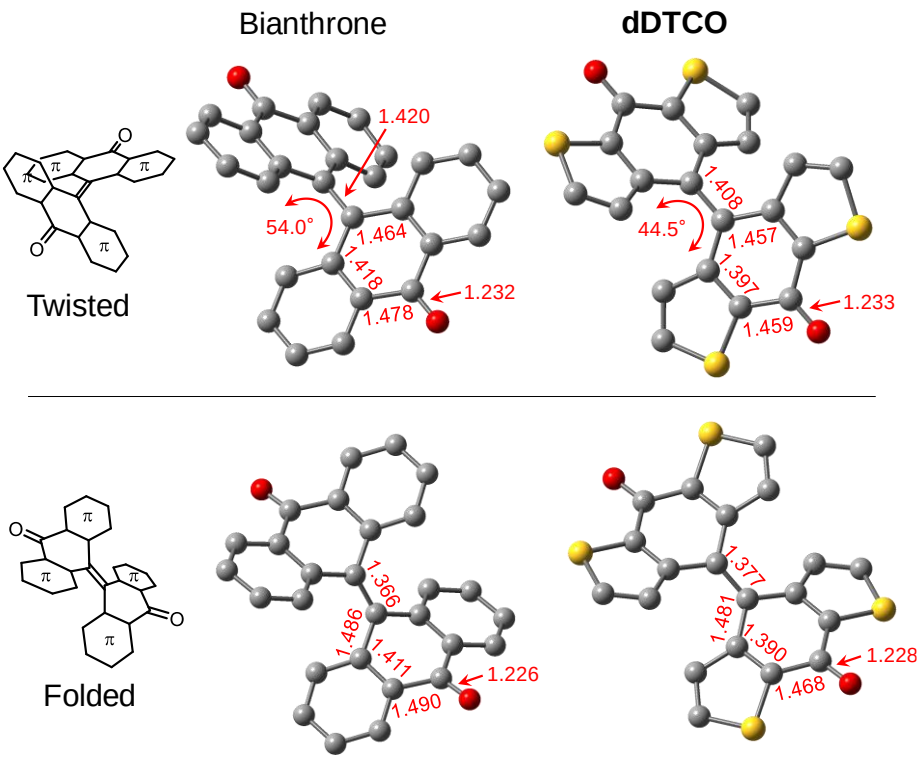

Figure S9 DFT-optimized twisted and folded conformers of bianthrone and **dDTCO** at the B3LYP/6-31G(d) level. Hydrogen atoms are omitted for clarity.

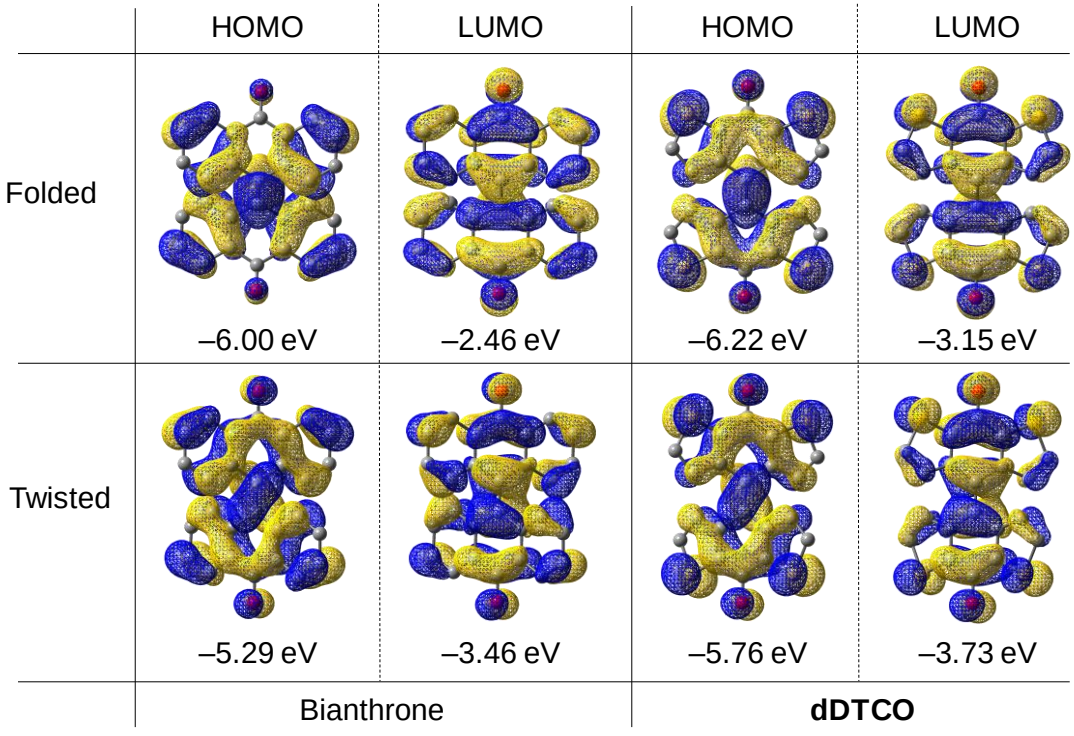

Fig. S10 Frontier molecular orbitals of aromatic-fused diphenoquinones calculated at the B3LYP/6-31G(d) level.

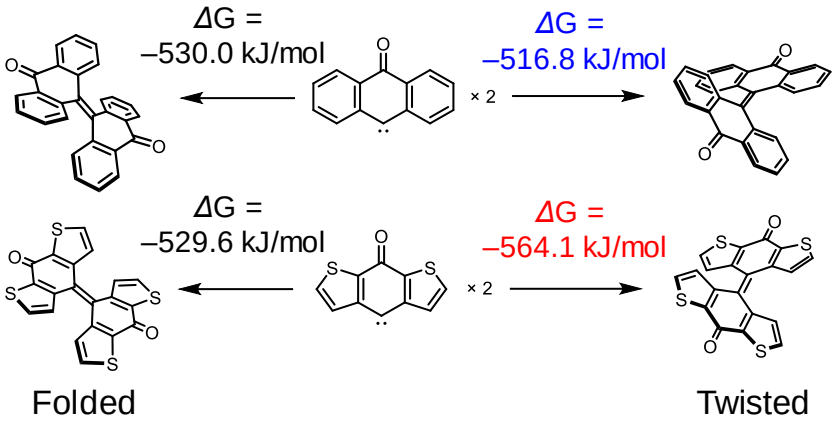

Fig. S11 Gibbs free energy differences for the formation of dimers from the corresponding singlet carbenes calculated by DFT at the B3LYP-D3BJ/6-31G(d) level.

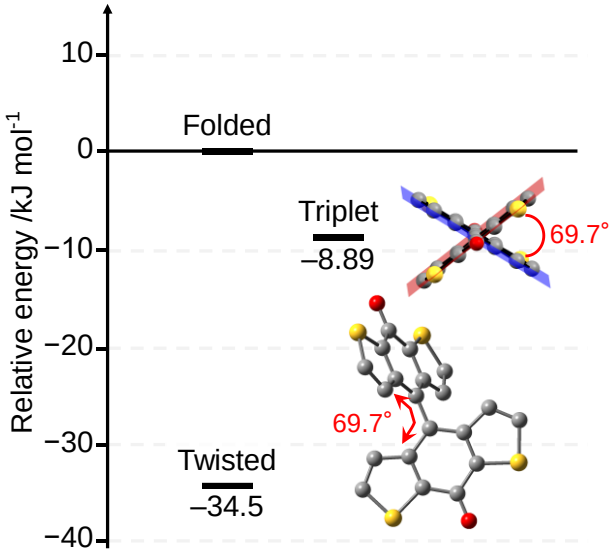

Fig. S12 Optimized triplet state structure of **dDTCO** with Gibbs free energy diagram at the B3LYP-D3BJ/6-31G(d) level at 298 K. The Gibbs free energy of the folded conformer is set at zero. Hydrogen atoms are omitted for clarity.

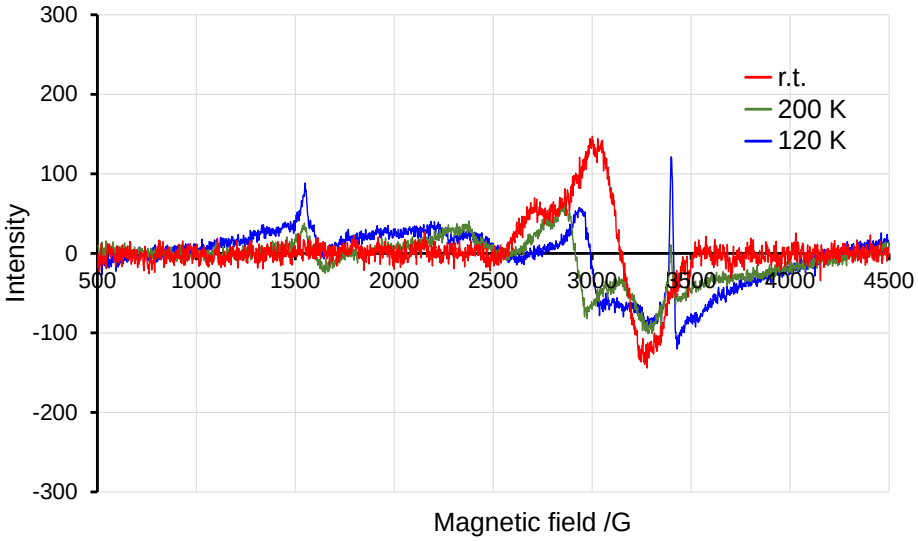

Fig. S13 ESR spectra of **dDTCO-Bu** in benzene at the concentration of 1 mM.

The ESR spectral lineshape at 200 K and 120 K were characteristic of the triplet state where a half-field absorption was clearly observed. The signals were not observed at 77 K. Therefore, the observed ESR signal is assigned to the excited triplet state of **dDTCO-Bu**.

Table S2 TD DFT results of the twisted conformer of **dDTCO** at the B3LYP/6-31G(d) level. Minor contributions are omitted for clarity.

Excited State	Composition	Contribution /%	Excitation energy /eV	Wavelength /nm	Oscillator strength
S0→S1	H-3→L	6	2.07	599	0.42
	H→L	97			
	H←L	5			
S0→S6	H-5→L	18	2.95	420	0.15
	H-3→L	74			
	H→L	7			
S0→S7	H-7→L	98	2.99	415	0.03
S0→S9	H-8→L	98	3.27	379	0.09
S0→S11	H→L+3	97	4.13	300	0.03

Table S3 TD DFT results of the folded conformer of **dDTCO** at the B3LYP/6-31G(d) level. Minor contributions are omitted for clarity.

Excited State	Composition	Contribution /%	Excitation energy /eV	Wavelength /nm	Oscillator strength
S0→S1	H-6→L	2	2.82	440	0
	H-1→L	96			
S0→S2	H-3→L	9	2.83	438	0.42
	H→L	91			
S0→S3	H-5→L	3	2.87	431	0.01
	H-2→L	95			
S0→S7	H-3→L	89	3.43	361	0.16
	H→L	8			
S0→S10	H-8→L	95	3.83	324	0.07
	H-1→L+1	4			
S0→S11	H-8→L	3	4.16	298	0.22
	H-1→L+1	92			

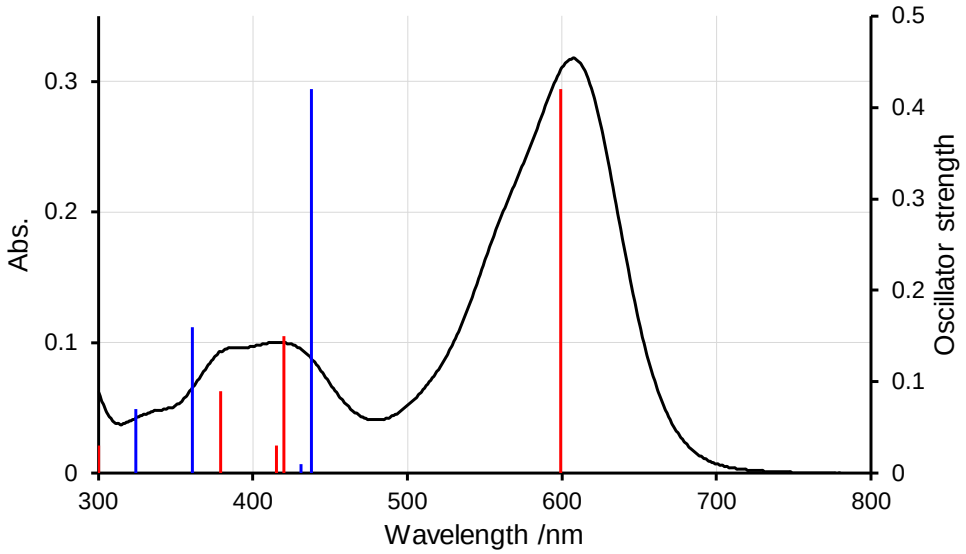

Fig. S14 Experimental absorption spectrum in CH_2Cl_2 (black line) and calculated TD-DFT results of twisted (red) and folded (blue) conformers at the B3LYP/6-31G(d) level for **dDTCO**.

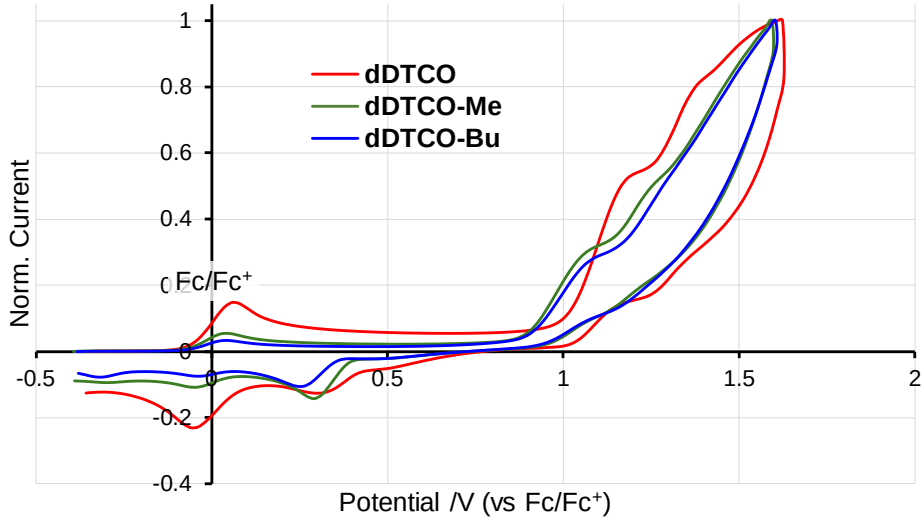

Fig. S15 Anodic cyclic voltammetry data of diphenoquinones in dichloromethane containing 0.1 M Bu_4NPF_6 at the scan rate of 100 mV s^{-1}.

Table S4 OFET characteristics of **dDTCO-Bu** and **dDTCO**.

Compound	μ_e /cm^2 V^{-1} s^{-1} [a]	V_{th} /V [b]	$I_{on/off}$ [c]
dDTCO-Bu	5.0×10^{-4}	39.0	1.3×10^5
	$[4.1 \times 10^{-4} \pm 9.4 \times 10^{-5}]$	[37.3 ± 2.6]	$[1.1 \times 10^5 \pm 8.0 \times 10^4]$
dDTCB	2.0×10^{-3}	35.2	1.3×10^5
	$[1.8 \times 10^{-3} \pm 2.4 \times 10^{-4}]$	[33.3 ± 1.7]	$[8.9 \times 10^4 \pm 3.5 \times 10^4]$

[a] Maximum electron field-effect mobility. Average mobilities of 5 cells with standard deviation are shown in parentheses. [b] Threshold voltage. [c] Current on/off ratio.

NMR and mass spectra

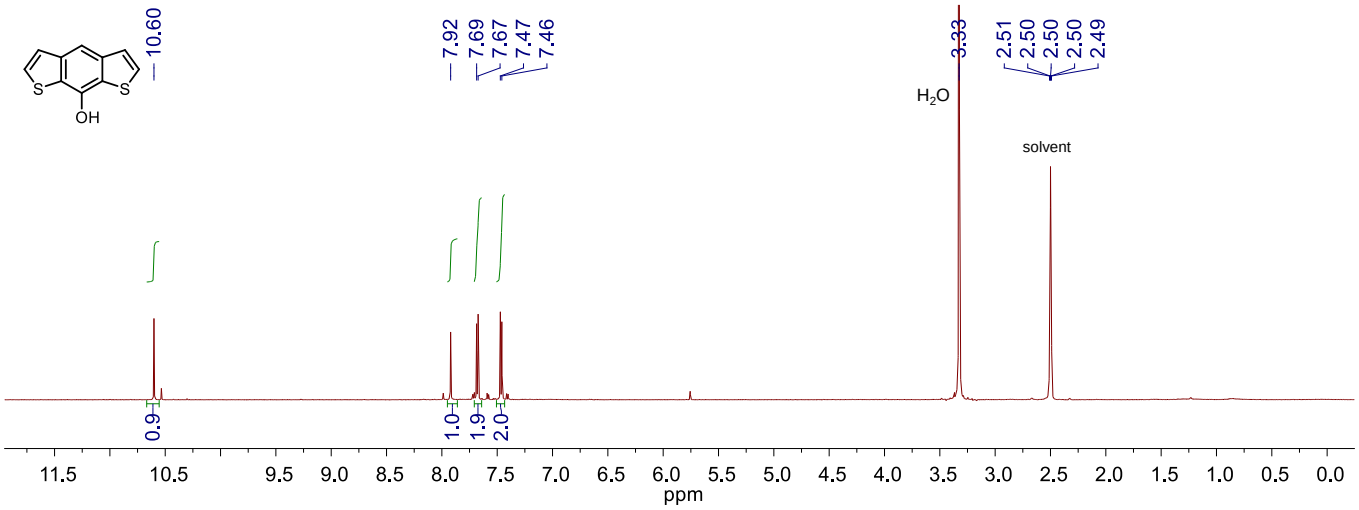

Figure S16 ^{1}H NMR spectrum of **DTCO** in DMSO-d_6 at room temperature (400 MHz).

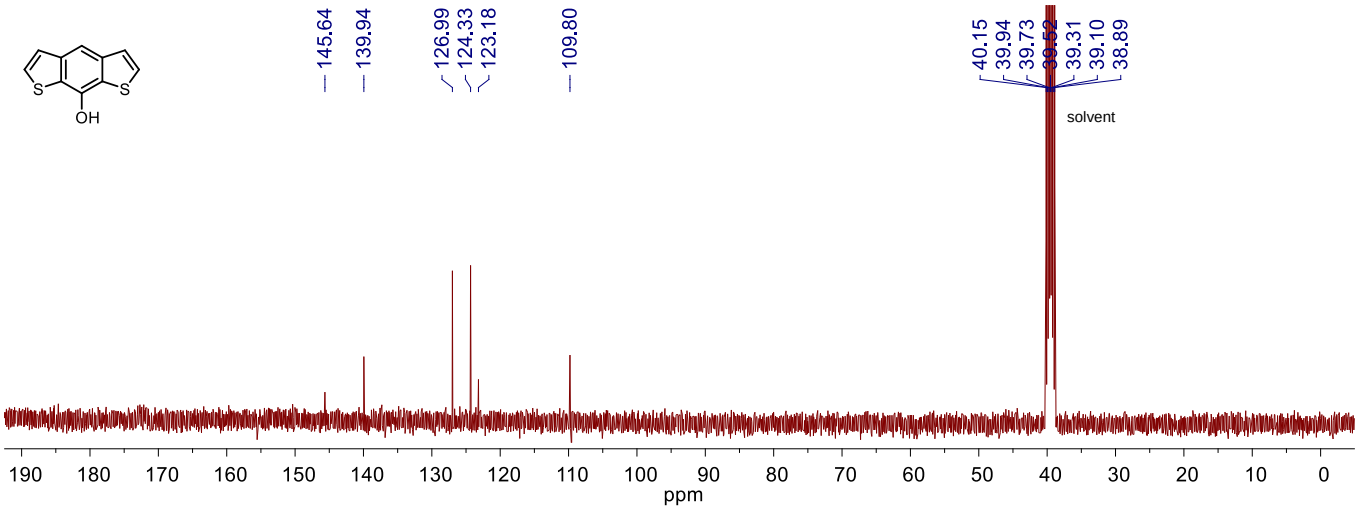

Figure S17 ^{13}C NMR spectrum of **DTCO** in DMSO-d_6 at room temperature (101 MHz).

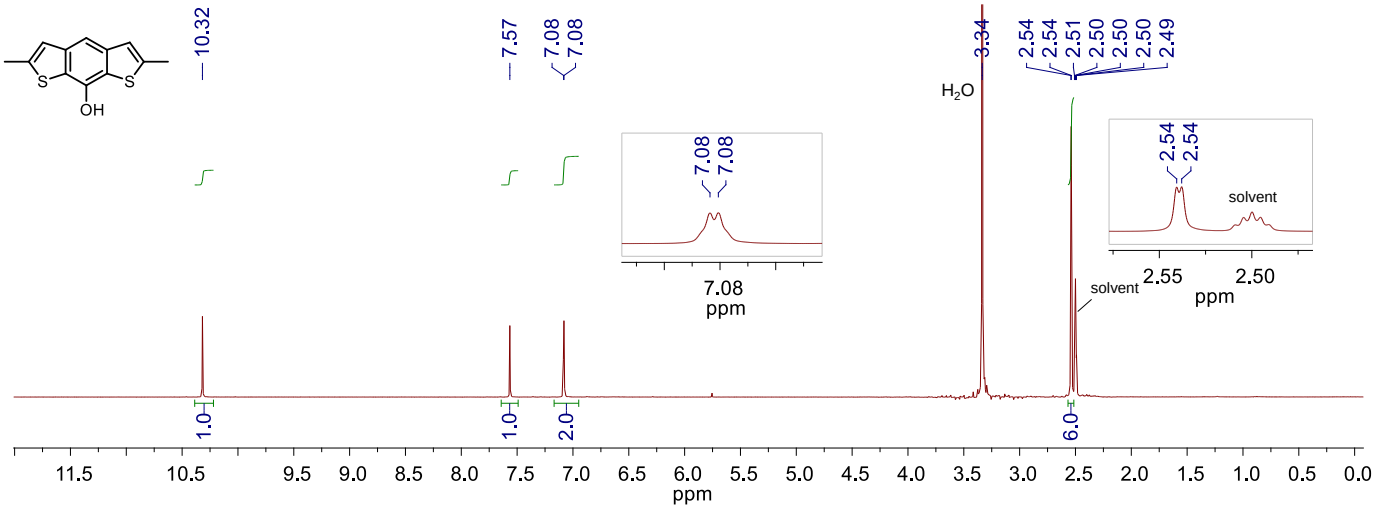

Figure S18 ^{1}H NMR spectrum of **DTCO-Me** in DMSO-d_6 at room temperature (400 MHz).

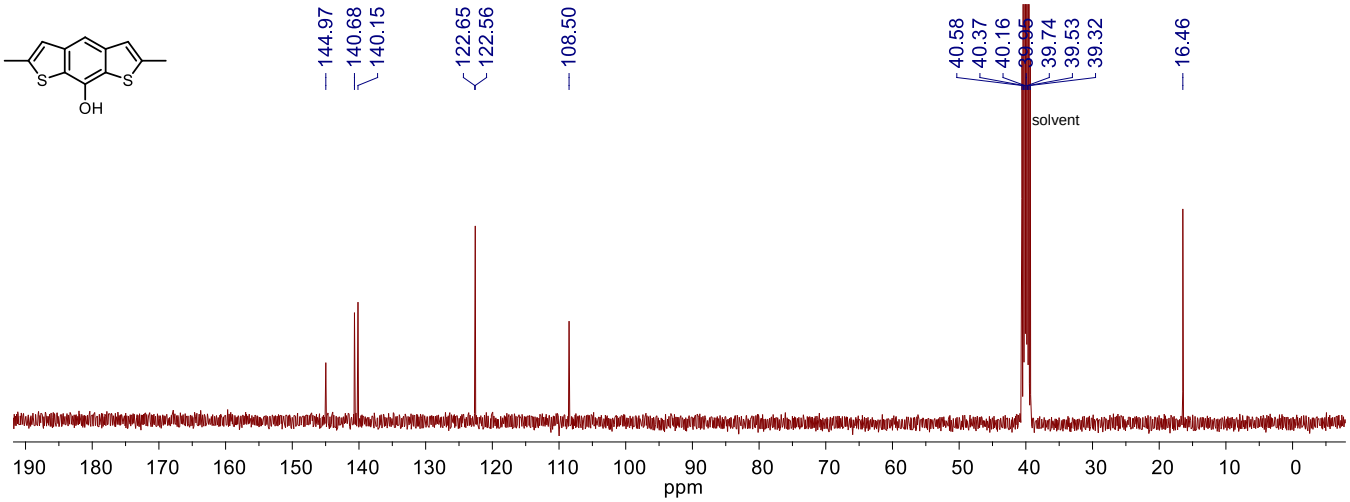

Figure S19 ^{13}C NMR spectrum of **DTCO-Me** in DMSO-d_6 at room temperature (101 MHz).

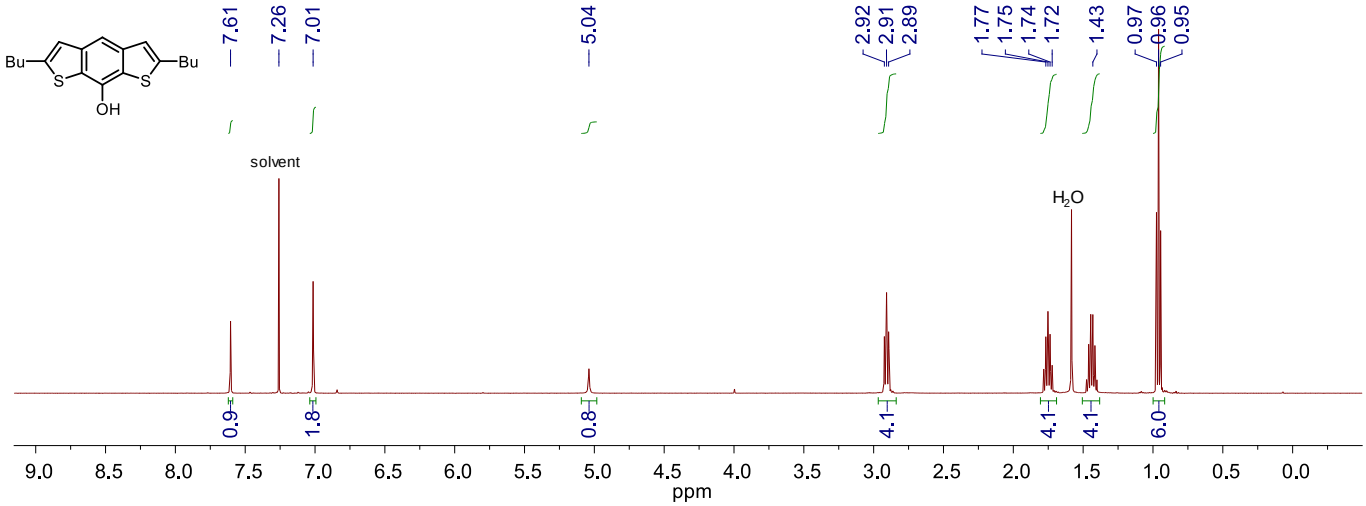

Figure S20 ^{1}H NMR spectrum of **DTCO-Bu** in $CDCl_3$ at room temperature (500 MHz).

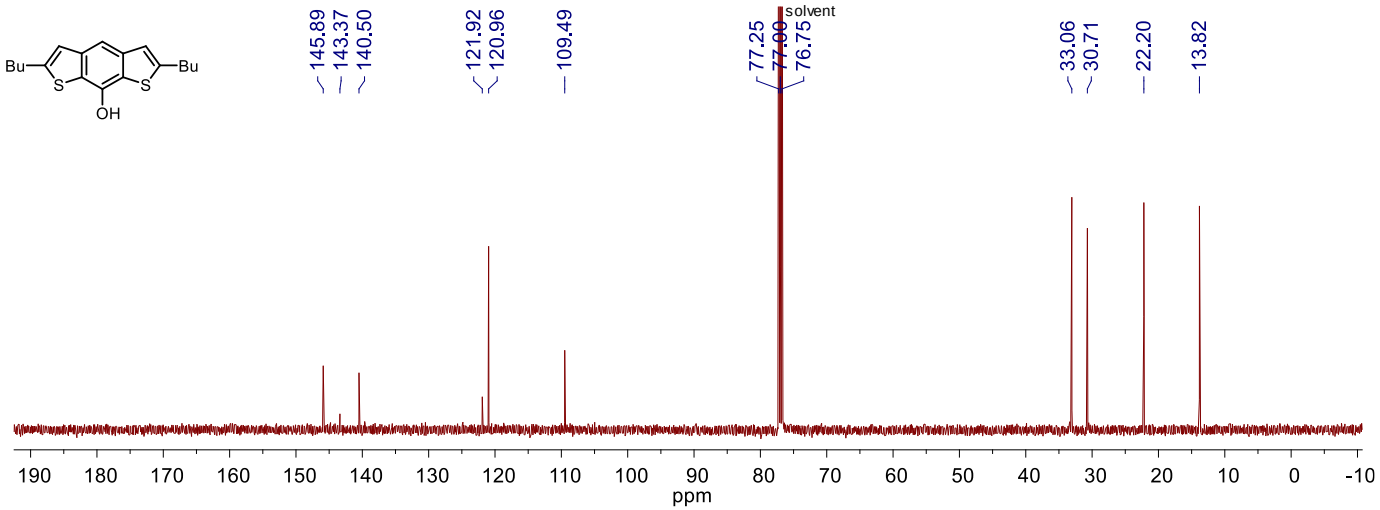

Figure S21 ^{13}C NMR spectrum of **DTCO-Bu** in $CDCl_3$ at room temperature (126 MHz).

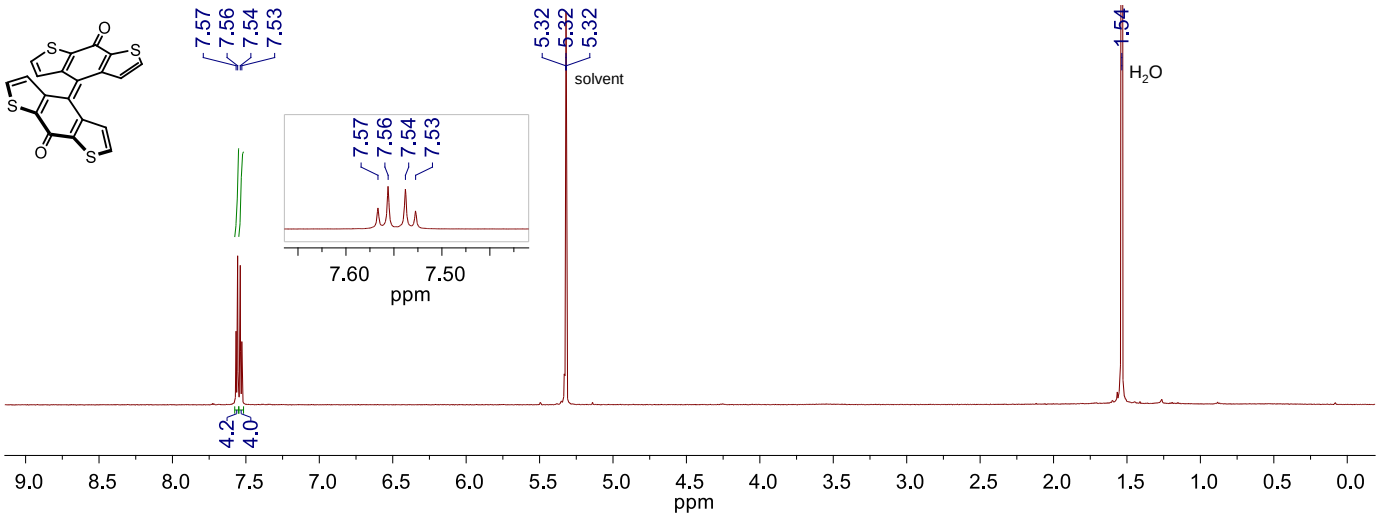

Figure S22 ^{1}H NMR spectrum of **dDTCO** in CD_2Cl_2 at room temperature (500 MHz).

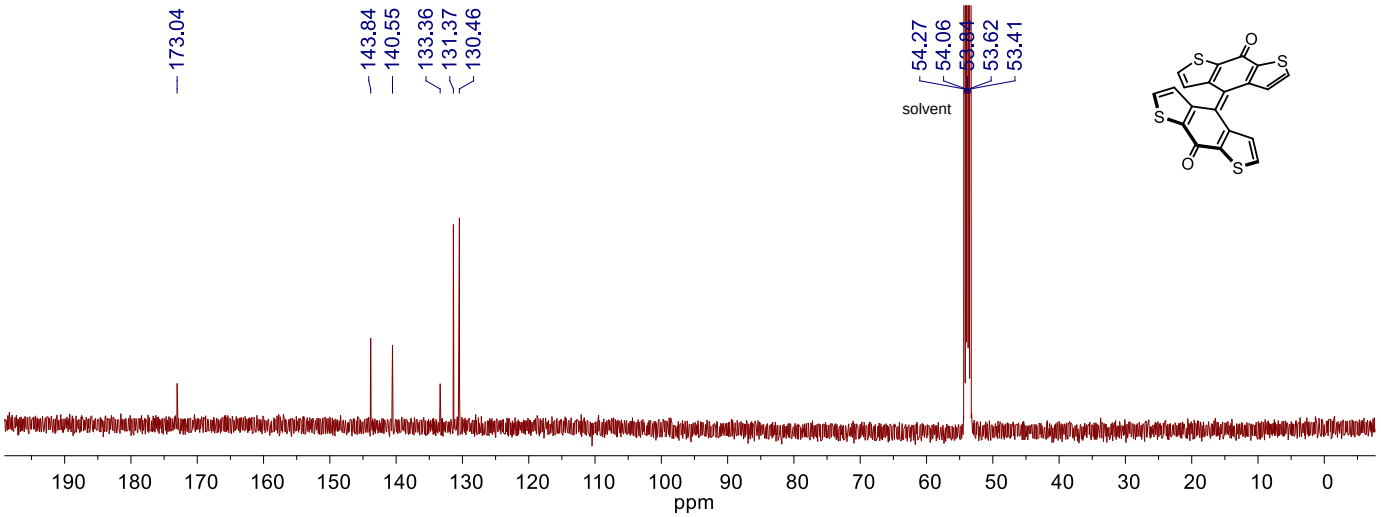

Figure S23 ^{13}C NMR spectrum of **dDTCO** in CD_2Cl_2 at room temperature (126 MHz).

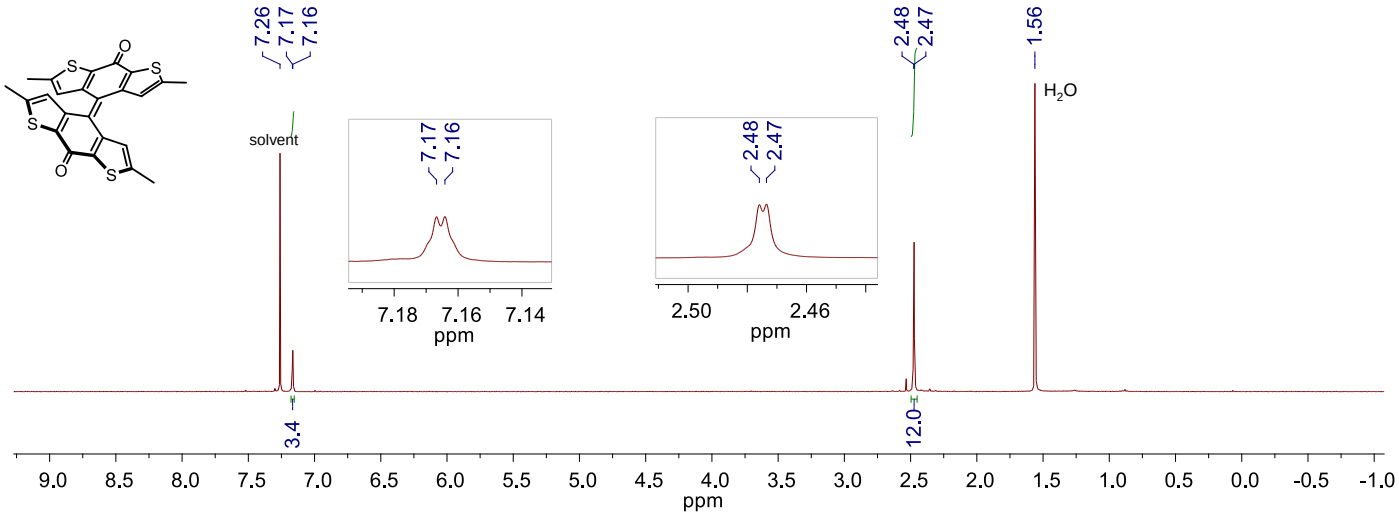

Figure S24 ^{1}H NMR spectrum of **dDTCO-Me** in $CDCl_3$ at room temperature (400 MHz).

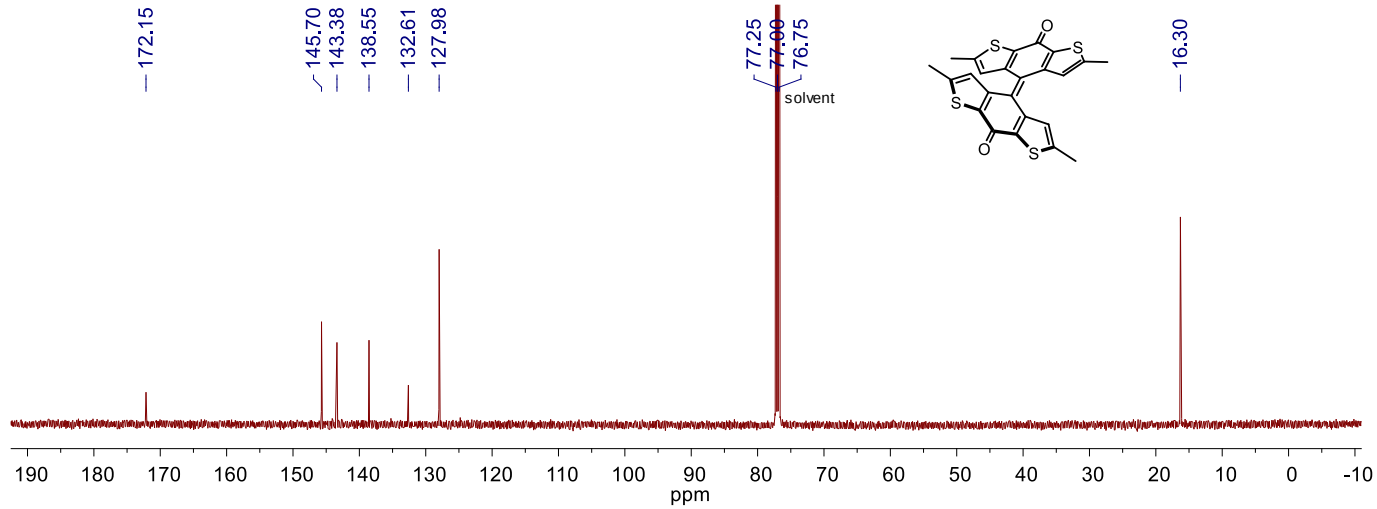

Figure S25 ^{13}C NMR spectrum of **dDTCO-Me** in $CDCl_3$ at room temperature (126 MHz).

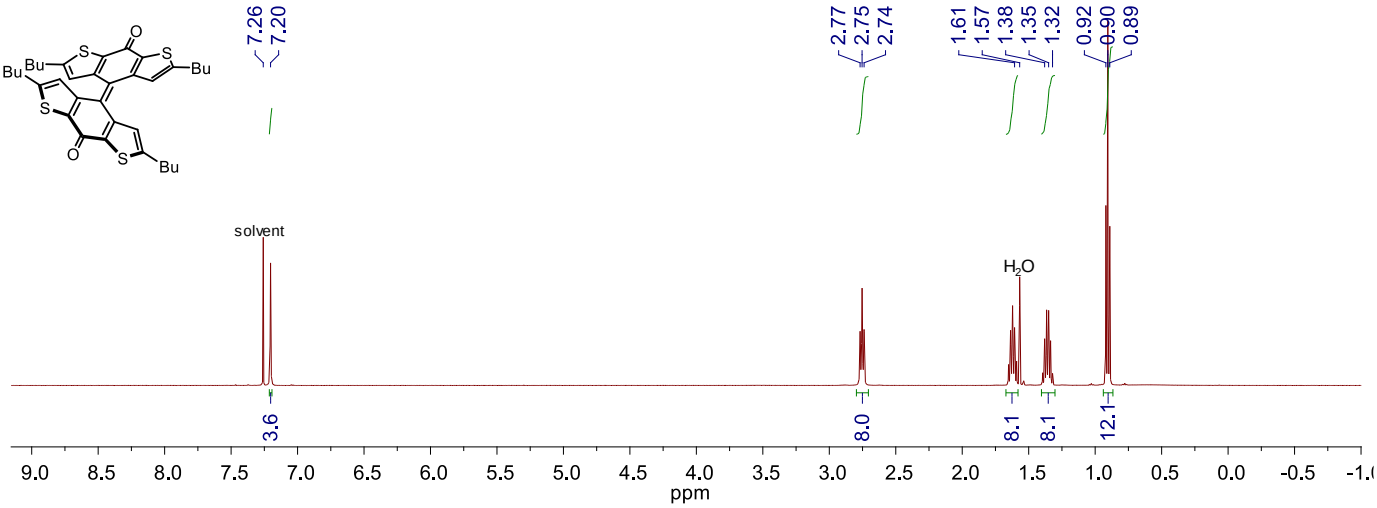

Figure S26 ^{1}H NMR spectrum of **dDTCO-Bu** in $CDCl_3$ at room temperature (500 MHz).

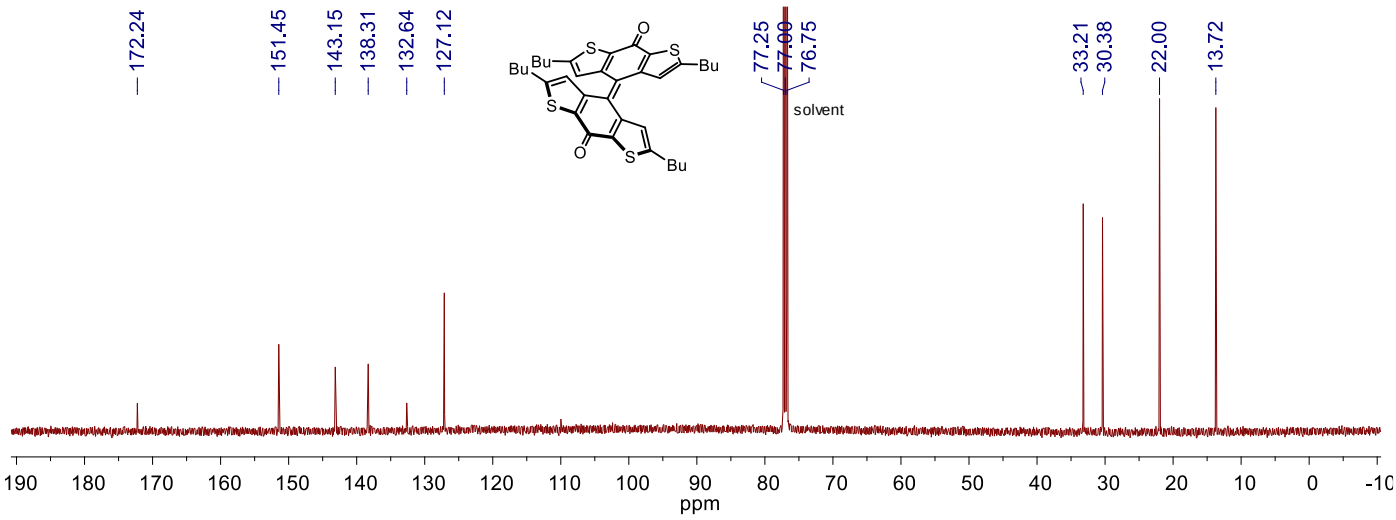

Figure S27 ^{13}C NMR spectrum of **dDTCO-Bu** in $CDCl_3$ at room temperature (126 MHz).

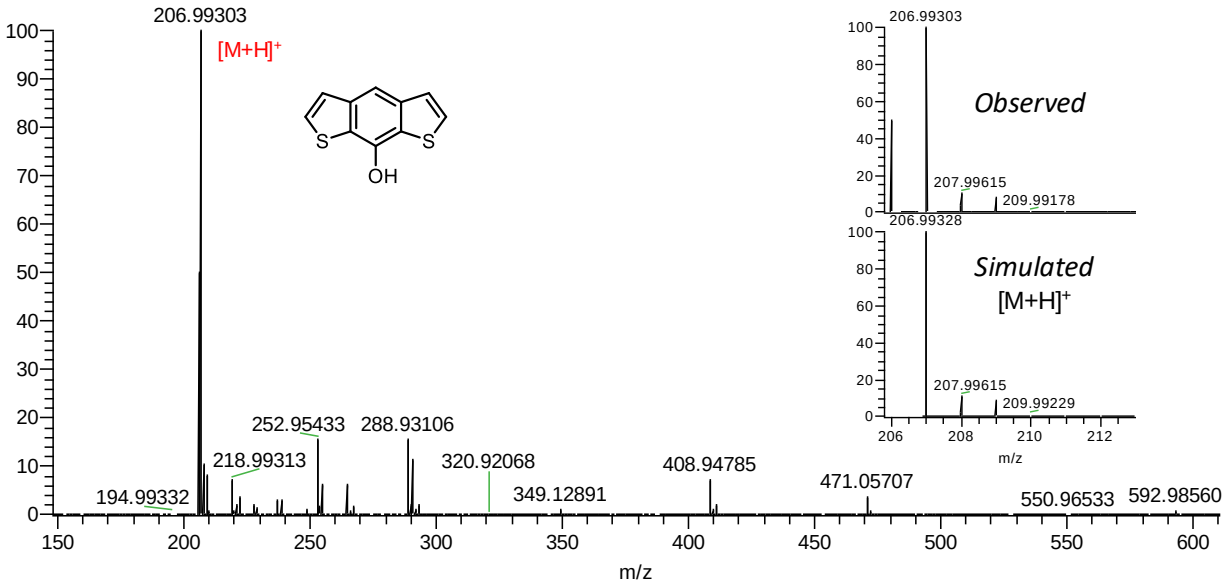

Figure S28 HR-APCI mass spectrum of **DTCO** (positive mode).

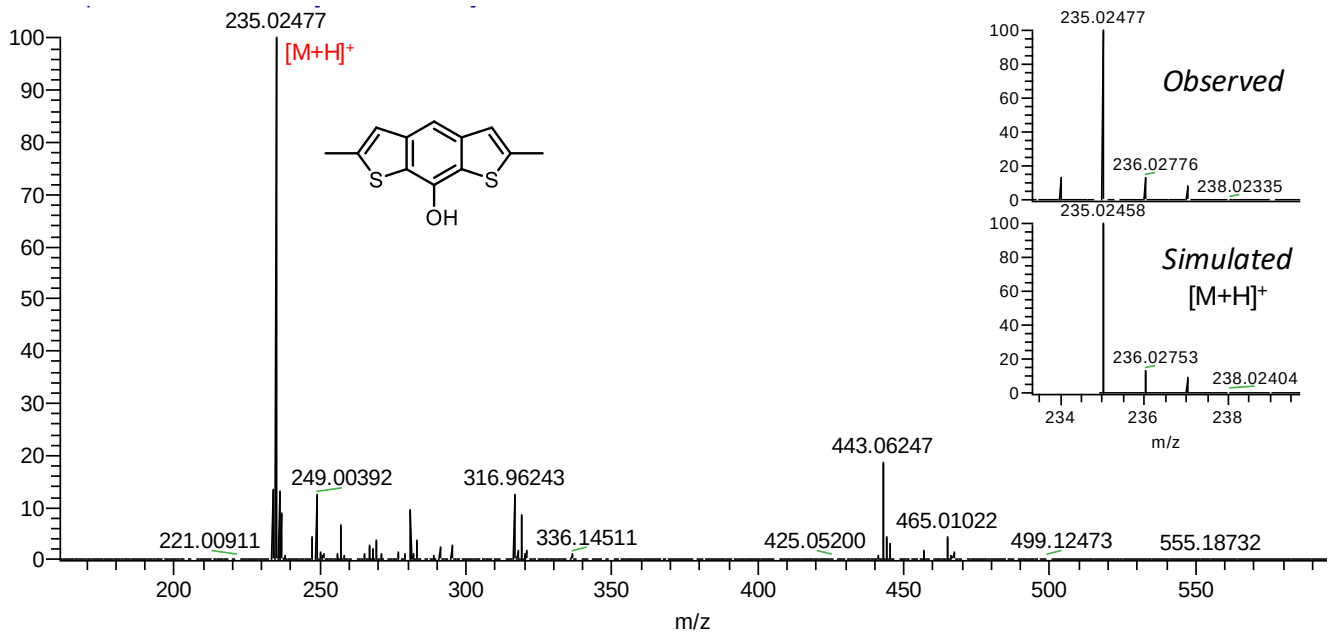

Figure S29 HR-APCI mass spectrum of **DTCO-Me** (positive mode).

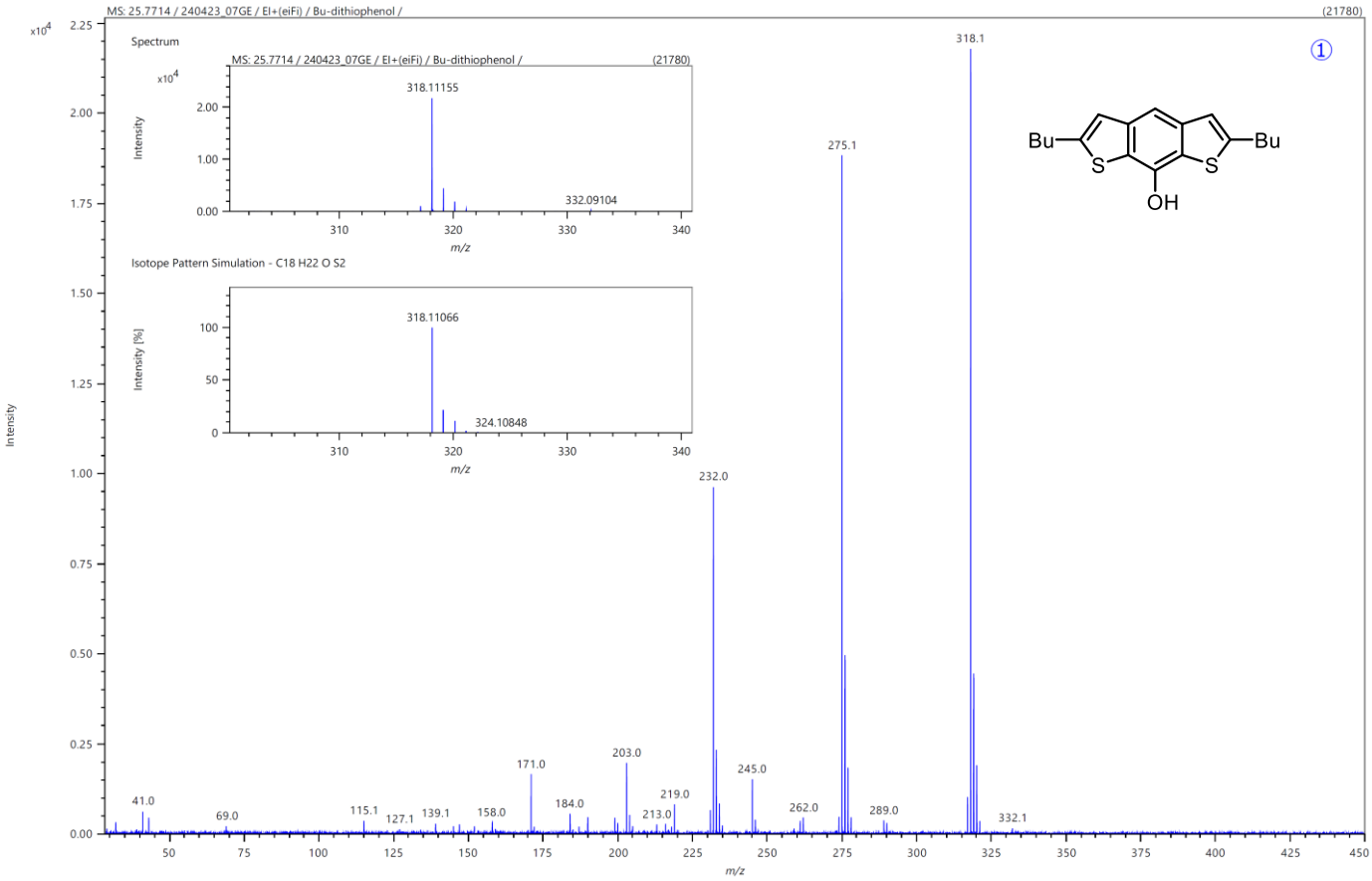

Figure S30 HR-GC-EI mass spectrum of **DTCO-Bu**.

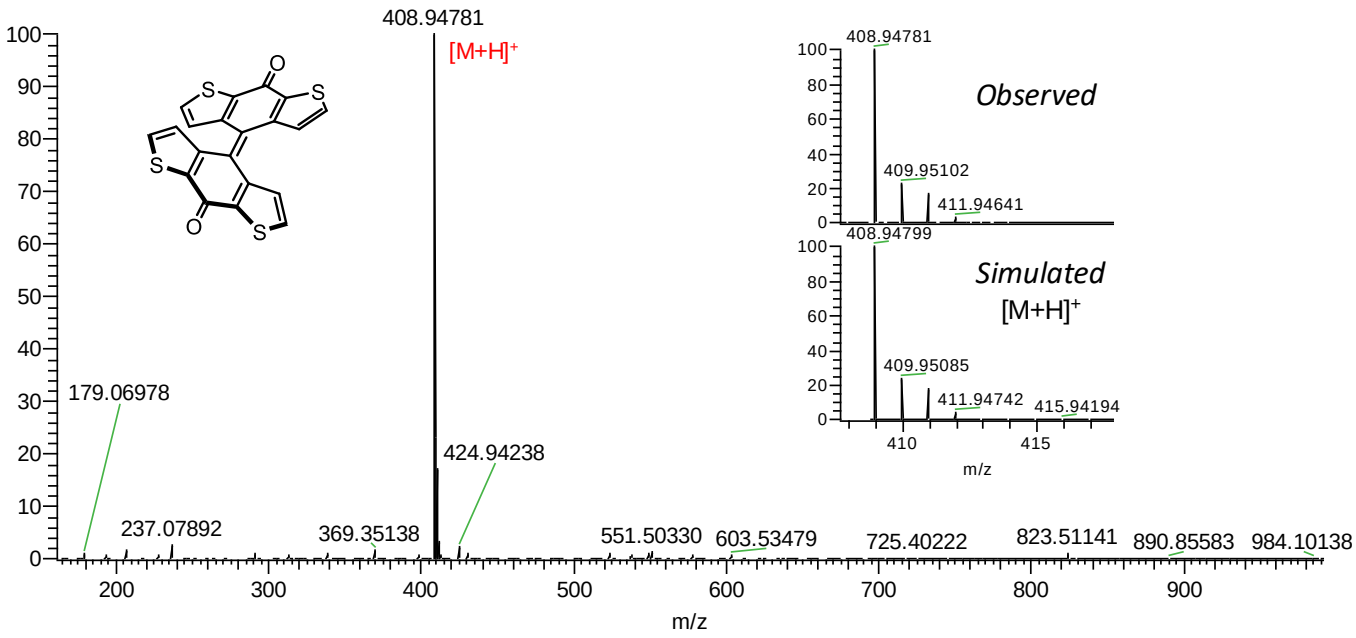

Figure S31 HR-APCI mass spectrum of **dDTCO** (positive mode).

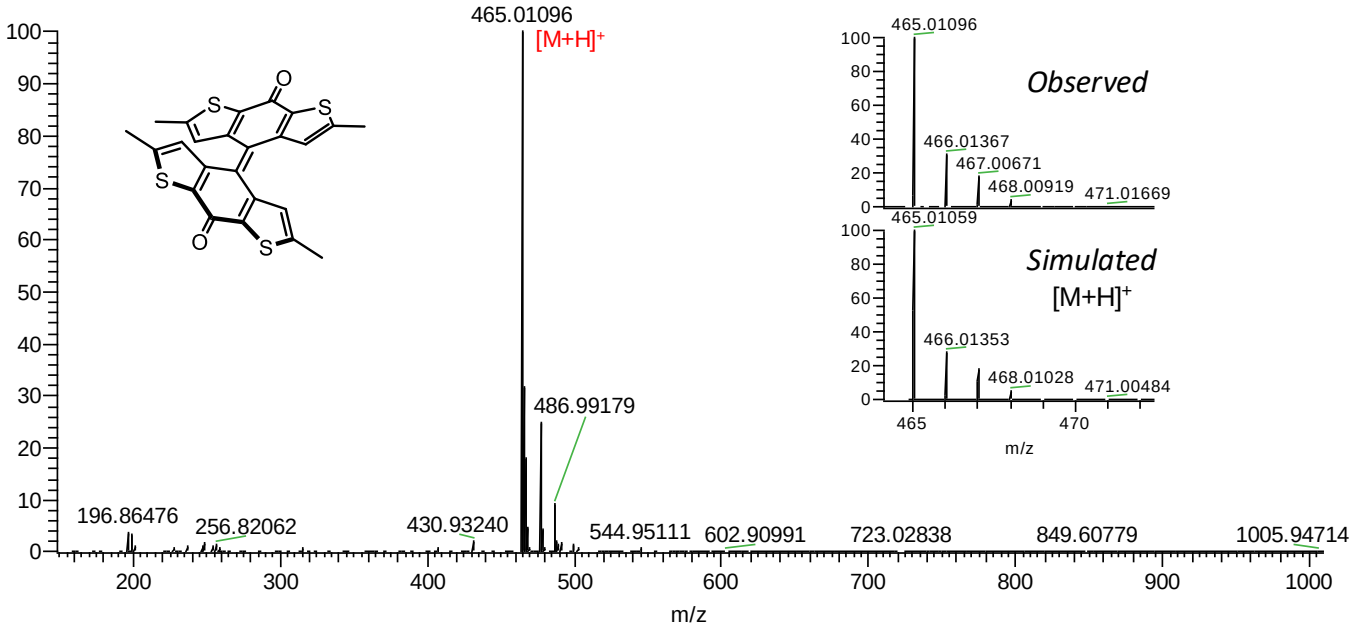

Figure S32 HR-APCI mass spectrum of **dDTCO-Me** (positive mode).

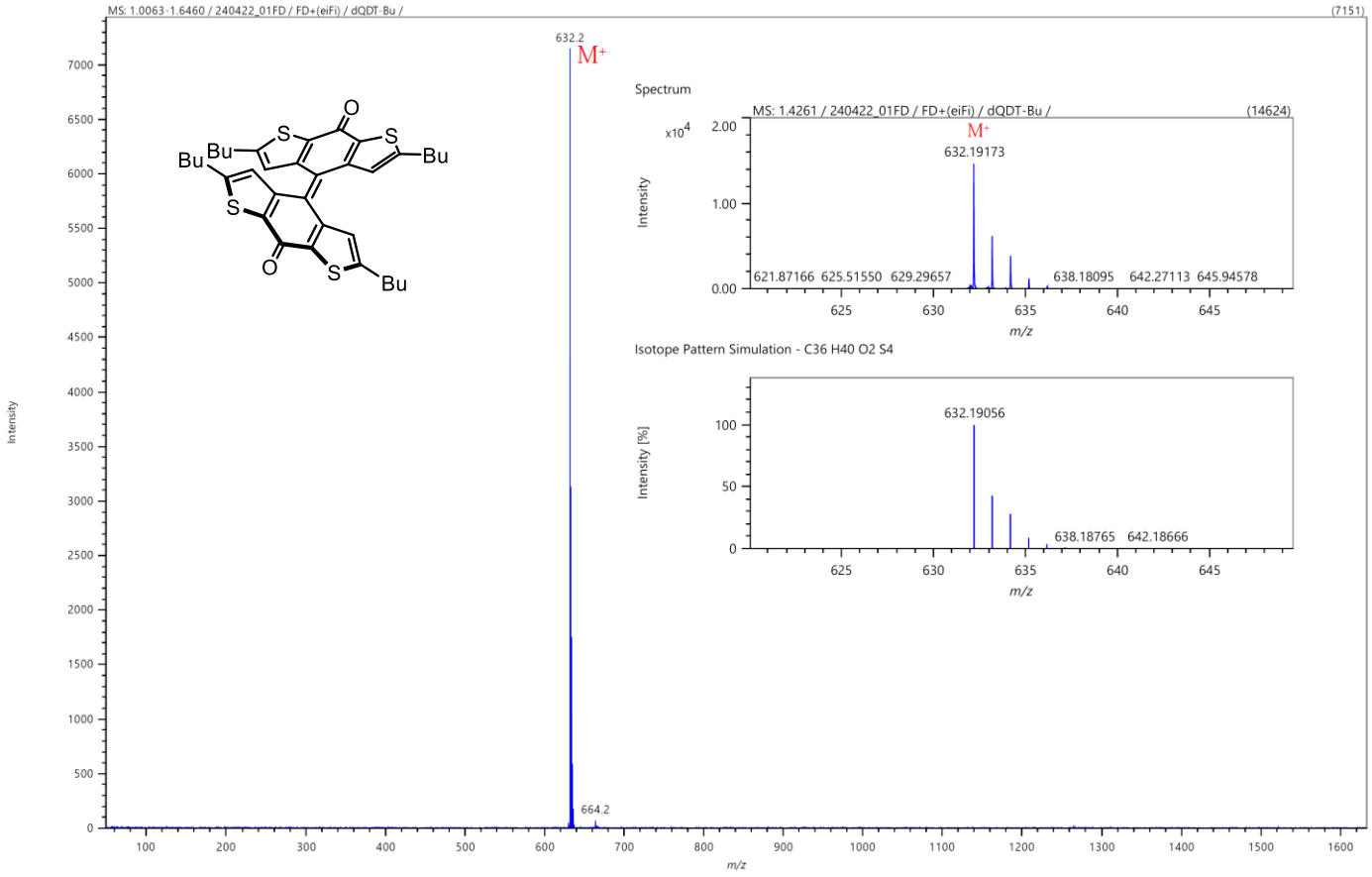

Figure S33 HR-GC-EI mass spectrum of **dDTCO-Bu**.